Ground-based Auroral Hiss Recorded at Northern Finland with Reference to Magnetic Substorms

J. Manninen[1], N. Kleimenova[2, 3], A. Kozlovsky[1], Yu. Fedorenko[4], L. Gromova[5], T. Turunen[1]

[1]Sodankylä Geophysical Observatory, Sodankylä, Finland

[2]Schmidt Institute of Physics of the Earth RAN, Moscow, Russia

[3]Space Research Institute RAN, Moscow, Russia

[4]Polar Geophysical Institute, Apatity, Russia

[5]Pushkov Institute of Terrestrial Magnetism, Ionosphere and Radio Wave Propagation RAN, Moscow, Troitsk, Russia

Correspondence to: J. Manninen (jyrki.manninen@sgo.fi)

Key Points:

- We analyze auroral hiss occurrence at ground-based auroral Finnish station Kannuslehto (KAN, MLAT = 64.2^{O}N) during 98 isolated magnetic substorms;
- The growth phase of 93% of substorms was accompanied by auroral hiss at KAN;
- Auroral VLF hiss observed in the equatorial region of the auroral oval (KAN location) is a typical signature of the substorm *growth* phase

Abstract

VLF auroral hiss at Kannuslehto (KAN), Finland has been analyzed with a reference to progress of 98 isolated magnetic substorms. During 11 winter months of 2015-2018, 91 of them were accompanied by the auroral hiss during the substorm growth phase. No auroral hiss was recorded during the expansion and recovery phases. We found auroral hiss was observed under rising polar cap PC index showing an increasing input of the solar wind energy into the magnetosphere during the substorm growth phase. We also found that KAN was mapped to the vicinity of enhanced Field Aligned Currents (FACs) during the auroral hiss occurrence. For the first time, it was established that the auroral VLF hiss generation in the equatorial part of the auroral oval (KAN location) is a typical signature of a substorm *growth* phase.

Plain Language Summary

Auroral hiss is a well-known type of nighttime natural VLF emission with a noise-like structure generated by the Cherenkov instability of precipitating soft electrons above the ionosphere. The auroral hiss (up to 39 kHz) occurrence in the equatorward region of the auroral oval at the Finnish station Kannuslehto (KAN, MLAT = 64.2^{O}N) was studied during the 11 winter months in 2015-2018. In this time interval, the 98 isolated and rather powerful magnetic substorms were recorded at Scandinavia. It was revealed that in the growth phase of the 91 substorms (i.e., 93% of all events of substorm), there was auroral VLF hiss observed at KAN simultaneously with an enhancement of Field Aligned Currents (FAC) exhibiting the soft electron precipitation which could be a plausible source of the auroral VLF hiss generation. For the first time, it was found that the auroral VLF hiss occurrence in the equatorward region of the auroral oval (KAN location) is a typical signature of the substorm growth phase.

1 Introduction

Auroral hiss is one of prominent natural whistler-mode VLF emissions (Helliwell, 1965) which have a noise-like structure and are commonly recorded both by the ground-based instruments and on board satellites throughout the auroral latitudes in the evening and nighttime (e.g., reviews by Makita, 1979; Sazhin et al., 1993; LaBelle and Treumann, 2002). Auroral hiss-like emissions have been recently found in Saturn magnetosphere by the Cassini spacecraft as well (Ye et al., 2016; Sulaiman et al., 2018).

The name ‘auroral hiss’ has been proposed by Martin et al. (1960) due to its connection with the visible aurora present somewhere in the sky and a hissing sound. Many early papers demonstrated a correlation between auroral hiss and visible auroras (e.g., Burton and Boardman, 1934; Ellis, 1957; Martin et al., 1960; Jørgensen and Ungstrup, 1962; Morozumi, 1965; Ungstrup, 1966; Harang, 1969) and it has found that this correlation is certainly not one-to-one. The hiss intensity and auroral luminosity were often not correlated (Martin et al., 1960; Jørgensen and Ungstrup, 1962; Jørgensen, 1966; Rosenberg, 1968, Labelle and Treumann, 2002) noting that these two phenomena are generated at different altitudes by different mechanisms and, possibly, by different electron populations. Moreover, aurora could be observed without auroral hiss (e.g., Srivastava, 1976).

It is believed that auroral hiss emissions are generated above the ionosphere at ~5000-20000 km by the Cherenkov instability at the frequencies above the lower hybrid frequency and below the electron plasma frequency or gyrofrequency, whichever is lower (Brice and Smith, 1965; McEwen and Barrington, 1967; Jørgensen, 1968; Maggs, 1976). Auroral hiss refers to downward electron beams with energies of ~100 eV - 1 keV (e.g., Gurnett and Frank, 1972; Hoffman and Laaspere, 1972; Laaspere and Hoffman, 1976). The low-altitude spacecrafts observed auroral hiss on the night-side almost every time when the spacecraft crossed the auroral zone (Gurnett, 1966; Barrington et al., 1971). Only a small fraction of VLF hiss

recorded by satellites reaches the ground. For example, Gurnett (1966) found only two auroral hiss events of 140 conjunctions occurred simultaneous on the ground and spacecrafts. Only waves with the wave normal angle within a narrow vertical transmission cone can penetrate the ionosphere to reach the ground level. The model (Sonwalkar and Haricumar, 2000) explains how auroral hiss can penetrate to the ground due to wave scattering by meter-scale *F* region density irregularities.

Auroral hiss observed on the ground is a fairly localized phenomenon, and is not simultaneously occurred at the stations with about 5° difference in latitude (e.g., Jørgensen, 1966; Srivastava, 1976). Moreover, Harang and Larsen (1965) showed a significant difference between auroral hiss observed at Tromsø and Kiruna stations separated by ~250 km. The similar result was reported by Makita (1979) and Nishino et al. (1982) comparing auroral hiss at Syowa and Mizuho stations separated by 260 km along the magnetic meridian. But at the same latitude, auroral hiss could be observed simultaneously at two sites spaced in longitude by at least about 400 km, for instance at Syowa and Molodezhnay stations in Antarctica (Kleimenova and Golikov, 1980) and at Kannuslehto in Finland and Lovozero in Russia (Manninen et al., 2018; Lebed et al., 2019).

Most the early studies of the auroral hiss properties have been based on the high-latitude VLF observations: Syowa at ~-70° MLAT and Mizuho at ~-72° MLAT (e.g., Tanaka et al., 1976; Makita, 1979; Sato et al., 1980; Nishino et al., 1982; Ozaki et al., 2008), Bird at ~-71° MLAT (Martin et al., 1960), South Pole at ~-74° MLAT (Spasojevic, 2016). Some knowledge of auroral hiss was obtained from auroral latitudes also, e.g., at Tromsø (~67° MLAT) (Harang and Larsen, 1965; Harang, 1968; Jørgensen, 1966), at Macquarie Island (~-65° MLAT) (Dowden, 1961), at Farewell, Alaska (~62° MLAT) (Morgan, 1977) and some others. Unfortunately, there were no simultaneous observations of auroral hiss at high- and auroral latitudes as the ocean is located at latitudes lower than Syowa and the sea is located poleward from the Scandinavian mainland auroral stations as well.

Many authors reported that auroral hiss is usually closely correlated with local geomagnetic activity, however, this statement is ambiguous. In particular, Jørgensen and Ungstrup (1962) did not find such correlation in Greenland VLF data, but Harang and Larsen (1965) showed a positive correlation between auroral hiss occurrence at the auroral latitudes and local moderate geomagnetic disturbances and negative one in the case of strong disturbances. Based on the Syowa observations, Makita (1979) (on page 88) claimed “most of auroral hiss emissions, including impulsive and continuous hiss are observed during the expansion phase of a substorm”, but Kokubun et al., 1972 reported some events of auroral hiss at Syowa observed in the substorm growth phase. However, at the lower, i.e., auroral latitudes, the auroral hiss occurrence in respond to substorm progress could be different.

It is well known that a magnetospheric substorm (first introduced by Akasofu, 1964) is one of the major agents in the coupling of the solar wind and magnetosphere, therefore, the understanding of a sequence of different geophysical phenomena during a substorm progress is one of the key problems in near-Earth space plasma physics. The aim of this paper is to study the substorm effects in the occurrence of auroral hiss at the auroral latitudes (at MLAT < ~ 70°).

2 Observations and discussion

Our study is based on the ground VLF observations at Kannuslehto (KAN) station (MLAT= 64.2°N) in Northern Finland. Several wintertime VLF campaigns (2006-2019) have been carried out at this remote, low industrial noise site. The VLF emissions are received by two orthogonal magnetic loop antennas, oriented in the geographic North-South and East-West directions, in the frequency band of 0.2-39 kHz sampled at 78.125 Hz (Manninen, 2005). The noise level of the receiver is about of 10^{-14} nT^2 Hz^{-1}. The method of the receiver calibration is

described in (Fedorenko et al., 2014). The Fast Fourier Transform (FFT) is performed to calculate the power spectral densities of the magnetic field of VLF emissions (frequency-time dynamic spectra, so called spectrograms).

Our observations are essentially different from the VLF registration method previously applied at Syowa and many other stations, there were used the chart paper records in several narrow bands (from 4 to 128 kHz) with different sensitivity at different frequencies (e.g., Makita, 1979). Our continuous records are also different from the VLF records at South Pole station used the 1 min digital data stored synoptically every 15 min (Spasojevic, 2016).

We have to underline, that our ground-based VLF measurements at KAN are carried out at much lower magnetic latitude than Syowa and South Pole Antarctic stations, so our recordings are badly hampered by well-known strong sferics (atmospherics) which hided all VLF emissions above ~3 kHz, especially during the night-time. Sferics are electromagnetic pulses originated from lightning discharges and propagate over distances of thousands of km inside the Earth-ionosphere waveguide (e.g., Volland, 1995). Therefore, to study high-frequency auroral hiss, we have to apply the special method of digitally filtering out the impulsive sferics with the duration less than 30 ms. The method has been briefly described in Manninen et al. (2016). Two examples of non-filtered and the filtered spectrograms are given in Figure 1. One can clearly see that the auroral hiss bursts became visible only after the sferics filtering.

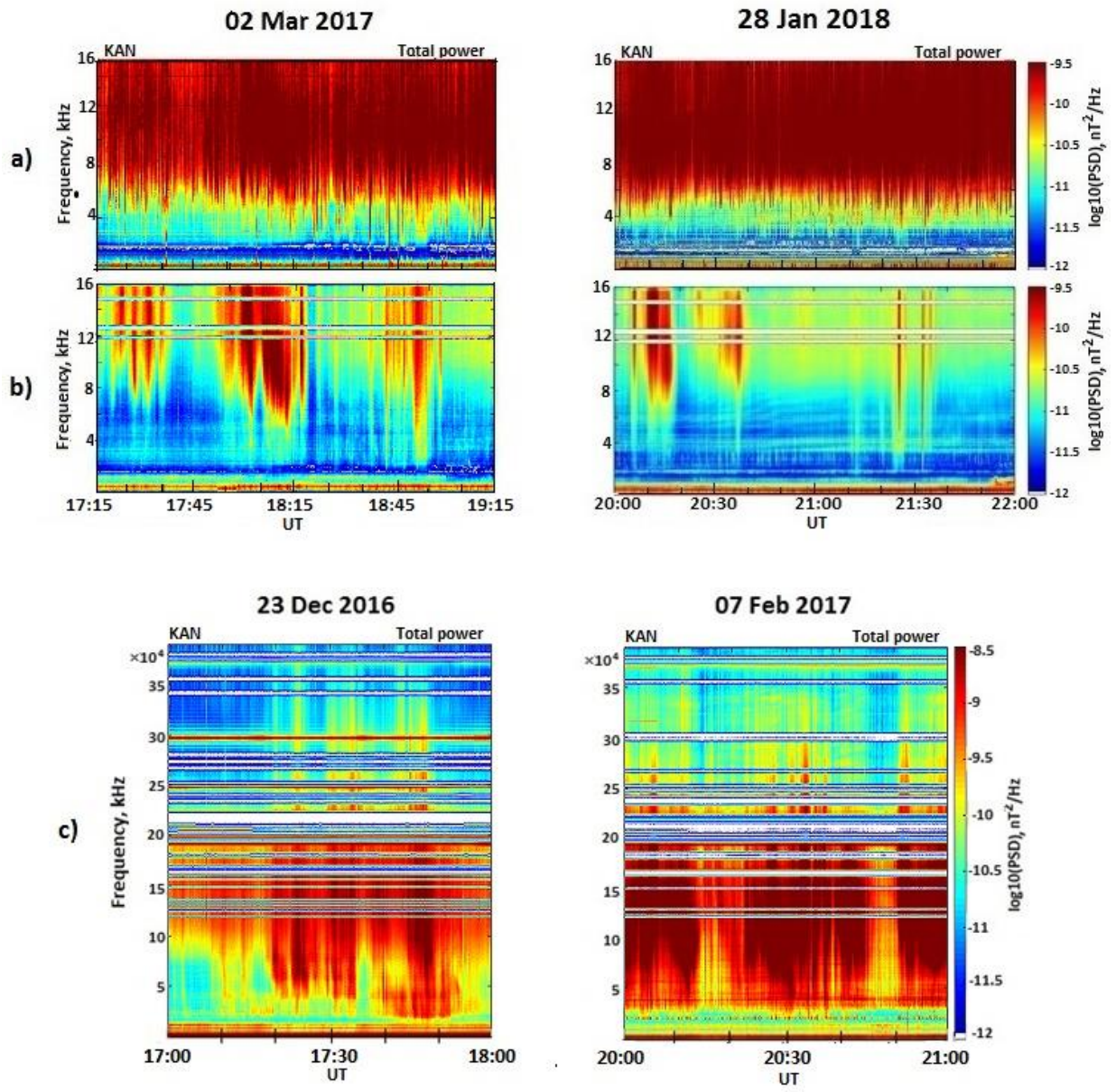

Fig. 1. Two examples of the VLF spectrograms at KAN. From top to bottom: a) nonfiltered spectrograms demonstrating how sferics hide all high-frequency VLF emissions; b) the same spectrograms after sferics filtering, the white horizontal lines are navigation transmitter signals after filtering; c) the auroral hiss spectrograms up to 39 kHz at KAN demonstrating auroral hiss bursts with intensity maximum concentrating around 10-15 kHz.

In the early works *(e.g., Morozumi, 1965; Kokubun et al.,1972; Tanaka et al., 1976; Makita,* 1979; Tanaka and Nishino, 1988), the auroral hiss at high-latitude Syowa Station has been divided into two types: continuous hiss and impulsive hiss. The continuous hiss is limited by frequencies less than 30 kHz and remained steady over tens of minutes or more, it is mainly associated with a steady auroral arc located far poleward from the VLF receiver. The impulsive hiss extends in frequency to several tens of kHz up to 100 kHz with very rapid intensity decreasing with frequency and consists of highly-structured bursts lasting from a few seconds to a few minutes, and accompanied by auroral brightening near the zenith. In the paper by Nishino et al. (1982), these types were called the "narrow-band" hiss and "wide-band" hiss. Sometimes the both types were observed simultaneously. The intensity maximum of both types was observed at the same frequencies around 10 kHz and diurnal variations of both type occurrence show the similar tendencies. Due to that, in some later papers (e.g., Nishino et al.,

1982), the auroral hiss properties have been investigated at frequency at 8 kHz which includes both types of hiss.

Our VLF observations at KAN (up to 39 kHz) do not allow to distinguish a high-frequency part of auroral hiss to clearly identify the presence of the impulsive hiss like at the Syowa station. Moreover, the auroral arcs which are plausible source of continuous auroral hiss, observed at Syowa and Mizuho stations, are located far poleward, up to 1000 km distant from Syowa (Nishino et al., 1982). It is too far to be recorded at the latitudes like the KAN location. So, the similar continuous hiss described in (e.g., Makita, 1979) can be hardly observed at KAN located in the equatorward part of auroral oval.

The auroral hiss dynamic spectra (spectrograms) at KAN look like bursts (groups of signals) with a duration from a few min to ~20 min representing dense sequences of short impulse signals lasting less than ~5 min. Moreover, almost every hiss burst reaches the instrument frequency cutoff (39 kHz) and extends above it, as it is clearly shown in Figure 1c. Further we call these bursts of VLF emissions "auroral hiss" as in classical monograph by Helliwell (1965).

Auroral hiss was recorded at KAN in 207 days during 11 winter months in 2015-2018 (total number of campaign days was 334) and occurred dominantly prior the magnetic midnight, mostly at 21-22 MLT (18-19 UT). That is in good agreement with many early works (e.g., Harang and Larsen, 1965; Jørgensen, 1966; Morgan, 1977; Makita, 1979). As in all previous studies, auroral hiss at KAN represented the right-hand polarized waves indicating the station location not far (less than ~300-400 km) from the ionospheric wave exit area, as it was shown by some authors, e.g., Ozaki et al. (2008).

It was found that auroral hiss at KAN was typically observed under low and moderate geomagnetic conditions with $Kp < 3$. There was no auroral hiss during very quiet days with $Kp \leq 1$ (93 days) as well as during very disturbed time with $Kp > 4$ (34 days). We found that within 207 auroral hiss days, 170 events (82%) were associated with local moderate high-latitude magnetic activity (sometimes with very complicated temporal variations looking as a sequence of multiple bay-like disturbances) and hiss bursts were typically recorded *before* their onsets. Not all of these magnetic disturbances can be classified as a magnetic substorm.

To extract the pure effect of the substorm progress, in our analysis, we selected only disturbances demonstrated the *typical isolated substorm* signature. Similarly, to Janzhura et al. (2007) the following criteria have been applied for the selection of the *typical isolated* substorms: (1) the intensity of a negative magnetic bay is more than 400 nT, (2) the sudden sharp drop of the magnetic X component in the substorm onset is more than 150-200 nT, (3) during the 3 h prior to the onset, there are no magnetic disturbances stronger than 200 nT. So, we selected only rather powerful substorms. The planetary AL index is usually used as a proxy of the substorm intensity. Contrary to that, to measure the substorm activity at Scandinavia, we applied the IL indicator of the local magnetic activity at the IMAGE meridian (http://space.fmi.fi/IMAGE) instead of the planetary AL index. The IL indicator is a local analog of the global AL index and calculated by the same method (Tanskanen, 2009).

Within 334 days of VLF observations, there were found only 98 isolated substorms with the onset between 17 UT and 22 UT (i.e., in the time interval of auroral hiss occurrence at KAN) fitted to our criteria. Among these 98 substorms, the 91 events (93%) were accompanied by auroral hiss observed *prior* to the substorm onsets (i.e., within the substorm growth phase) as it is illustrated in Figure 2 (upper plot). Only a few auroral hiss bursts were observed within 10

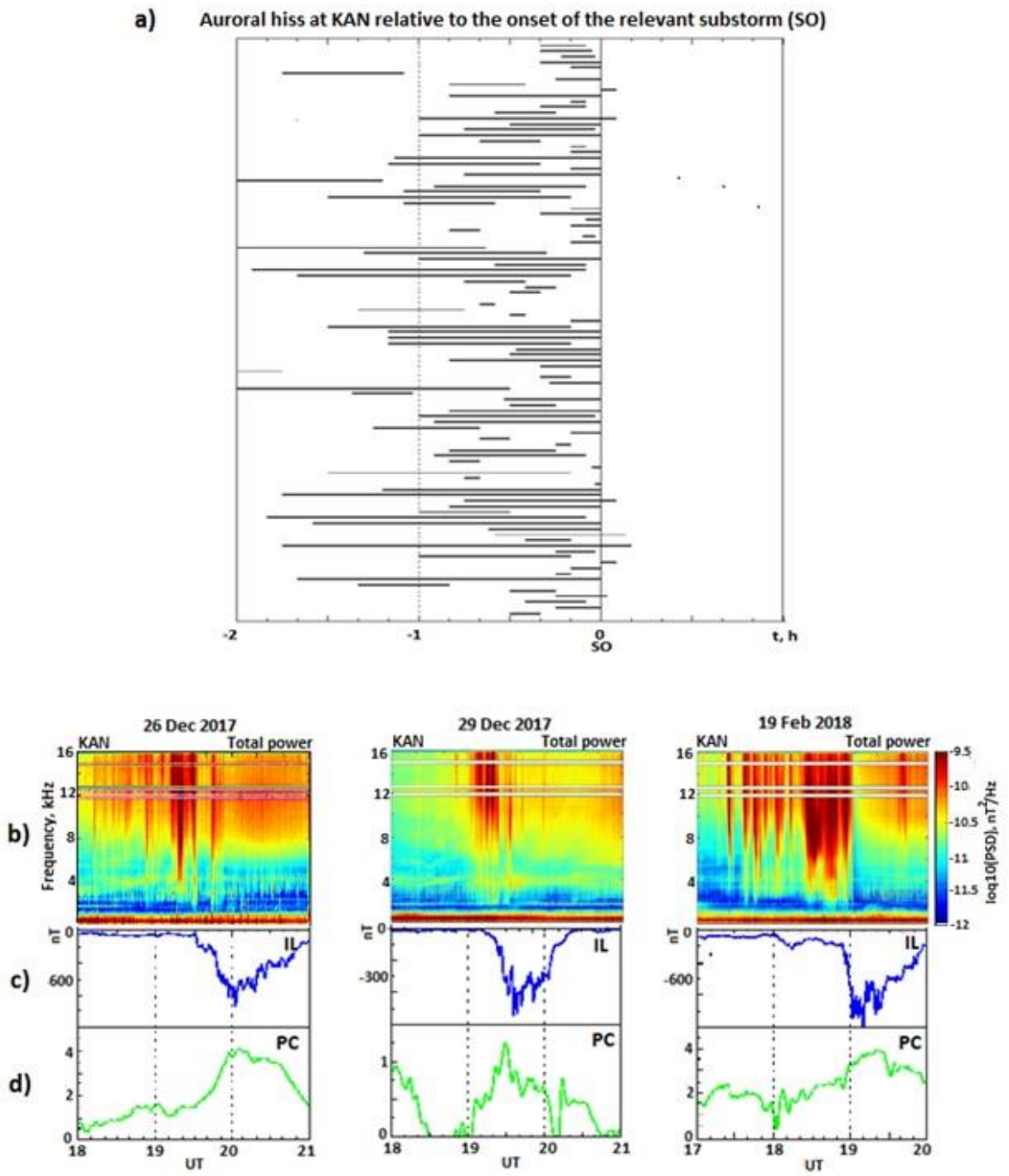

Fig. 2. Top panel (a): the plot of auroral hiss occurrence relatively to the onsets (SO) of the 91 magnetic substorms demonstrating the auroral hiss during the substorm growth phase and the sudden disappearance of these emissions within the substorm onset. Bottom panels: the examples of auroral hiss during the substorm progress: b) auroral hiss spectrograms; c) the IL indicator showing that the auroral hiss bursts are observed prior to the substorm onset; d) the polar cap PC index as a proxy of the input of the solar wind energy into the magnetosphere which increases in the substorm growth phase.

min after the substorm onset. No auroral hiss was recorded during the expansion and recovery phases of the studied substorms. The 7 events of substorms without auroral hiss were mostly caused by sudden jumps of the solar wind dynamic pressure and did not show the typical growth phase.

In Figure 2, it is clearly seen that auroral hiss disappeared in the time of the substorm onset. It could be a result of the VLF wave absorption caused by an enhancement of precipitating electrons in this time. But our study of the 30 MHz riometer absorption data (SOD) (http://www.sgo.fi), observed during and after the considered 91 substorm onsets, showed that the absorption higher than 1.5 dB (which can suppress hiss) was observed only in 27 events (~30% of the events). So, we may suppose that the sudden auroral hiss disappearance can be a result by not only the ionosphere VLF absorption, but, probably, by the shift of the auroral hiss source to the higher latitudes.

Thus, our finding shows that the auroral hiss recorded in KAN is a typical signature of the *growth* phase of a substorm. The concept of a growth phase existence prior to the magnetic substorm onset was discussed by several authors (e.g., Pudovkin et al., 1968; McPherron, 1970; Kokobun, 1971; Iijima and Nagata, 1972; Sergeev et al., 2011; Clausen et al., 2012), They demonstrated that substorm growth phase is accompanied by some magnetospheric phenomena, such as temporal activations of the pre-breakup quiet auroral arcs and their gradual equatorward shift, Pi2 geomagnetic pulsations, electron precipitation enhancement. The substorm growth phase is generally believed to be initiated by the southward turning of the Interplanetary Magnetic Field (IMF) (e.g., McPherron et al., 1973; Iyemori, 1980), and the increasing of an input of the solar wind energy into the magnetosphere (e.g., Li et al., 2013).

One of the indicators of these processes could be the polar cap PC index introduced by Troshichev et al. (1988) and Stauning (2013). The PC index is a proxy of the polar cap magnetic activity generated by the geoeffective interplanetary electric field and the southward IMF. A substorm can start only if the energy input into the magnetosphere exceeds an appropriate threshold of the energy storage. Troshichev et al. (2014) found that during the growth phase of a substorm, the PC index rises until it has reached some threshold level (~1.5 ± 0.5 mV/m) for a possible substorm onset.

We considered the behavior of PC index two hours prior and during the auroral hiss bursts observed before all 91 studied substorms accompanied by hiss. It was found that there was the common tendency to increasing of the values of the PC index prior and during the auroral hiss at KAN. But at times under the PC index general enhancement, some short-time decreasing of the PC index could be observed. Usually it was a result of a short-time IMF variations, for instance, a northward turning of the IMF Bz. Figure 2 (bottom panels) displays 3 examples of the variations of the PC index and IL indicator during auroral hiss bursts. We found only 9 cases between 91 studied events when during auroral hiss occurrence, there were no PC index increasing, but before that, the PC index already reached the values 2.5-3.5 mV/m, required for a substorm development (Troshichev et al., 2014).

Since auroral hiss is caused by Cherenkov radiation of the low-energetic precipitating electrons, we considered the behavior of the upward Field Aligned Currents (FACs), also known as Birkeland currents, corresponded to the soft electron precipitation. Some upward current increasing prior to a substorm onset was found in Forsyth et al (2018).

To study the FACs during the auroral hiss occurrence at KAN, we used the global maps of FACs provided by AMPERE (Active Magnetosphere and Planetary Electrodynamics Response Experiment) facility which consists of the 66 telecommunication satellites at 780 km altitude

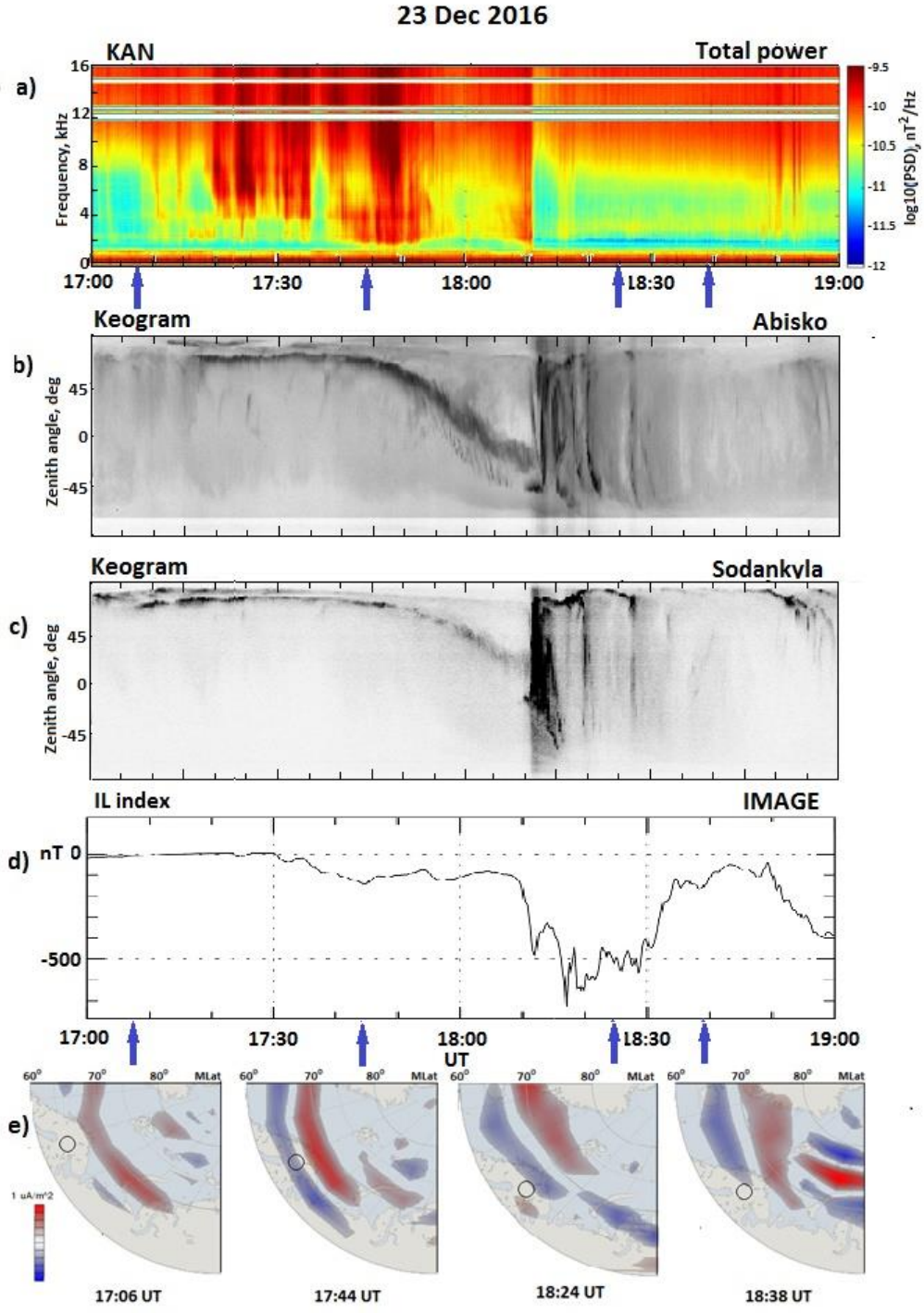

Fig. 3. Survey of the auroral hiss event on 23 December 2016 at 17-19 UT. From top to bottom: a) the auroral hiss spectrogram; b) the auroral keogram from Abisko; c) the auroral keogram from Sodankylä; d) the IL indicator of the magnetic activity; e) the South-West quarters of the global map (in geomagnetic coordinates) of the Field Aligned Currents (FACs) according to the AMPERE data (http://ampere.jhuapl.edu). Blue arrows point the time of these map of auroral hiss at KAN was accompanied by the upward FAC increasing in the pre-midnight sector. constructions. The upward FACs are marked by red and the downward FACs – by blue. The small circles indicate the location of KAN

(e.g., Anderson et al., 2014). Since the AMPERE data were available only up to 17 September 2017, we estimated (using the summary plots of the AMPERE maps in http://ampere.jhuapl.edu) the average location of the enhanced upward FACs during the events

of the auroral hiss occurrence in the growth phase of the considered 65 substorms in 2015-2017. It was found that in the 58 events, prior to the substorm onset (when auroral hiss was recorded at KAN), the enhanced upward FACs were located roughly at ~66-68° MLAT, and about 20-30 min after the substorm onset they shifted westward to ~71-73° MLAT (at that time the auroral hiss bursts at KAN disappeared). It is well known typical FAC dynamics during substorm progress (e.g., Sergeev et al., 2011; Clausen et al, 2012; Forsyth et al, 2018). We have to note that very often the upward FAC enhancement was observed without the auroral hiss occurrence, but each event

One typical auroral hiss event (at ~17:10-18:10 UT on 23 December 2016) is presented in Figure 3. In this event, the optical auroras were observed as keograms (zenith angles along the meridian of aurora versus time) at two stations: Abisko (ABK, MLAT= 65.4°N, located ~300 km to North-West from KAN) and Sodankylä (SOD, MLAT= 64.1°N, located ~37 km to South from KAN). Both keograms showed the same auroral arc poleward of these stations. The arcs moved equatorward after ~17.50 UT. The auroral breakup was observed at ~18:10 UT simultaneously with the sharp drop of the IL indicator and strong impulsive riometer absorption at Sodankylä up to 5 dB (not shown here). That completely suppressed auroral hiss. The maps of the FAC distribution according to the AMPERE data are shown in Figure 3e. Well before the substorm onset and in the absence of auroral hiss at KAN, the upward FACs were located far poleward from KAN. Together with the auroral arc moving, the FACs moved to the lower latitudes as well, and KAN became in the vicinity of the upward FACs. In the substorm expansion phase, after the 18:10 UT breakup, there was no auroral hiss at KAN, and the upward FACs shifted to the MLAT ~70°, far poleward from KAN. There were no auroral hiss in the substorm recovery phase, and the enhanced FACs were recorded far poleward from KAN.

3 Conclusion

The analysis of VLF auroral hiss observation during 11 winter months of 2015-2018 at KAN, (located in the auroral latitudes, at MLAT= 64.2°N) has been done with a reference to a substorm progress.

During these 11 winter months, the 98 isolated and rather powerful magnetic substorms were recorded at Scandinavian meridian by the IMAGE magnetometer network. It was revealed that the 91 substorms (93%) were accompanied by the auroral hiss bursts observed in the substorm *growth* phase. We also found that auroral hiss prior to a substorm onset was observed under rising values of the polar cap PC index showing an increasing of the input of the solar wind energy into the magnetosphere during the substorm growth phase. Besides, we found that before a substorm onset when the auroral hiss occurs, KAN was located in the vicinity of an enhancement of Field Aligned Currents (FAC) demonstrated the soft electron precipitation which could be a plausible source of the auroral hiss generation.

Thus, it was concluded that the typical wave signature of the substorm *growth* phase is auroral hiss generation at the auroral latitudes.

This result is not consistent with the data obtained at high-latitude Antarctic Syowa Station (MLAT ~70°S) where auroral hiss was mostly observed during the *expansion* phase of a substorm (Makita, 1979), although in some cases, auroral hiss was observed also during the substorm growth phase as well (Kokobun et al., 1972). This apparent contradiction may be a result of the space-temporal dynamics of the precipitation of low-energetic electrons and the correspondent high-latitude FACs during the substorm cycle: in the substorm *growth* phase, all geophysical processes develop in the auroral latitudes, while in the substorm *expansion* phase they move to much higher latitudes. The global maps of FAC distribution, constructed by the AMPERE facility data during the substorm cycle, demonstrated an excellent agreement with paradigm of the polar cap expansion of FACs after the substorm onset. The ground-based

feature of the auroral hiss at different latitudes is controlled by the space-temporal dynamics of a substorm progress.

Acknowledgments

The work of N.K., L.G. and Yu.F. was partially supported by the grants of Academy of Finland (for N.K.and L.G.no.308501, and no.294931 for Yu.F.), The filtered VLF KAN data are available at http://www.sgo.fi/pub_vlf/ as the power spectrograms in 24-h, 1-h and 1-min intervals for all campaigns 2006-2019. The IMAGE magnetometers and IL indicator data are available at http://www.space.fmi.fi/IMAGE. The auroral keograms were taken from http://www.space.fmi.fi/All_sky_cameras_of_MIRACLE. The AMPERE data are available at http://ampere.jhuapl.edu. We thank the AMPERE team and the AMPERE Science Center for providing the Iridium derived data products. The PC index values were provided by http://pcindex.org.

References

Akasofu, S.-I. (1964). The development of the auroral substorm. *Planetary and Space Science, 12*, 273–282. https://doi.org/10.1016/0032-0633(64)90151-5

Anderson, B. J., Korth, H., Waters, C. L., Green, D. L, Merkin, V. G, Barnes, R. J., & Dyrud, L. P. (2014). Development of large-scale Birkeland currents determined from the Active Magnetosphere and Planetary Electrodynamics Response Experiment. *Geophysical Research Letters*, *41*(9), 3017–3025. https://doi.org/10.1002/2014GL059941

Barrington, R. E., Hartz, T. R & Harvey, R. W. (1971). Diurnal distribution of ELF, VLF and LF noise at high latitudes as observed by Alouette 2. *Journal of Geophysical Research, 76*, 5278–5291. https://doi.org/10.1029/JA076i022p05278

Brice, N.M., & Smith, R.L. (1965). Lower hybrid resonance emissions. *Journal of Geophysical Research, 70*, 71–78. https://doi.org/10.1029/JZ070i001p00071

Burton, E.T., & Boardman, E.M. (1934). Audio-frequency atmospherics. *Transactions AGU, 15*(1), 155–158. https://doi.org/10.1029/TR015i001p00155

Clausen, L. B. N., Baker, J. B. H, Ruohoniemi, J. M., Milan, S. E., & Anderson, B. J. (2012). Dynamics of the region 1 Birkeland current oval derived from the Active Magnetosphere and Planetary Electrodynamics Response Experiment (AMPERE). *Journal of Geophysical Research, 117*, A06233. https://doi.org/10.1029/2012JA017666

Dowden, R. L. Simultaneous observations of VLF noise ('hiss') at Hobart and Macquarie Island (1961). *Journal of Geophysical Research, 66(5)*, 1587-1588. https://doi.org/10.1029/JZ066i005p01587

Ellis, G.R. (1957). Low frequency radio emissions from auroras. *Journal of Atmospheric and Solar - Terrestrial Physics, 10*, 302–306. https://doi.org/10.1016/0021-9169(57)90128-9

Fedorenko, Y., Tereshchenko, E., Pilgaev, S., Grigoryev, V., & Blagoveshchenskaya, N. (2014). Polarization of ELF waves generated during “beating-wave” heating experiment near cutoff frequency of the Earth-ionosphere waveguide. *Radio Science, 49*, 1254–1264. https://doi.org/10.1002/2013RS005336

Forsyth, C., Shortt, M., Coxon, J. C., et al. (2018). Seasonal and temporal variations of field-aligned currents and ground magnetic deflections during substorms. *Journal of Geophysical Research: Space Physics, 123*, 2696–2713. https://doi.org/10.1002/2017JA025136

Gurnett, D.A. (1966). A satellite study of VLF hiss. *Journal of Geophysical Research, 71*, 5599–5615. https://doi.org/10.1029/JZ071i023p05599

Gurnett, D.A., & Frank, L. A. (1972). VLF hiss and related plasma observations in the polar magnetosphere. *Journal of Geophysical Research, 77*, 172–190. https://doi.org/10.1029/JA077i001p00172

Harang, L., & Larsen, R. (1965). Radio wave emission in the VLF-band observed near the auroral zone. 1. Occurrence of the emissions during distubances, *Journal of Atmospheric and Terrestrial Physics., 27*(4), 481-497. https://doi.org/10.1016/0021-9169(65)90013-9

Harang, L. (1968). VLF emissions observed at stations close to the auroral zone and at stations on lower latitudes, *Journal of Atmospheric and Solar - Terrestrial Physics.*, *30*(6), 1143–1160. https://doi.org/10.1016/S0021-9169(68)80004-2

Harang, L. (1969). Radio noise from aurora, *Planetary Space Science*, *30*(7), 869–877. https://doi.org/10.1016/0032-0633(69)90093-2

Helliwell, R.A. (1965). Whistler and related ionospheric phenomena, Stanford, Stanford Univ. Press, 349 p.

Hoffman, R. A., & Laaspere, T. (1972). Comparison of very-low-frequency auroral hiss with precipitating low-energy electrons by the use of simultaneous data from two OGO 4 experiments. *Journal of Geophysical Research*, *77*, 640–650. https://doi.org/10.1029/JA077i004p00640

Iijima, T. & Nagata, T. (1972) Signatures for substorm development of the growth phase and expansion phase. *Planetary Space Science, 20*, 1095-1112. https://doi.org/10.1016/0032-0633(72)90219-X

Iyemori, T. (1980), Time Delay of the substorm onset from the IMF southward turning, *J. Geomagnetism and Geoelectricity, 32*, 267–273. https://doi.org/10.5636/jgg.32.267

Janzhura, A., Troshichev, O. & Stauning P. (2007), Unified PC indices: Relation to the isolated magnetic substorms. *Journal of Geophysical Research*, 112, A09207, https://doi.org/10.1029/2006JA012132.

Jørgensen, T. S., & Ungstrup, E. (1962). Direct observation of correlation between auroras and hiss in Greenland. *Nature*, *194*, 462–463. https://doi.org/10.1038/194462a0

Jørgensen, T. S. (1966). Morphology of VLF hiss zones and their correlation with particle precipitation events. *Journal of Geophysical Research*, *71*, 1367–1375. https://doi.org/10.1029/JZ071i005p01367

Jørgensen, T. S. (1968). Investigation auroral hiss measured on OGO-2 and Byrd station in terms of incoherent Cherenkov radiation. *Journal of Geophysical Research*, *73*, 1055–1069. https://doi.org/10.1029/JA073i003p01055

Kleimenova, N. G., & Golikov, Yu. V. (1980). Local peculiarities of auroral hiss observed in polar Antarctic regions. *Memories of National Institute of Polar Research. Special issue No 16*, 52-55

Kokubun, S. (1971). Polar substorm and interplanetary magnetic field. *Planetary Space Science, 19*, 697–714

Kokubun, S., Makita, K., & Hirasawa, T. (1972). VLF-LF Hiss During Polar Substorm. *Report of Ionosphere and Space Research in Japan, 26*, 138–148

Laaspere, T., & Hoffman, R. A. (1976). New results on the correlation between low-energy electrons and auroral hiss. *Journal of Geophysical Research*, *81*, 524–530. https://doi.org/10.1029/JA081i004p00524

LaBelle, J., & Treumann, R. (2002). Auroral Radio Emissions, 1. Hisses, Roars, and Bursts, *Space Science Reviews*, *101*(3), 295–440

Lebed, O. M., Fedorenko, Yu. V., Manninen, J., Kleimenova, N. G., & Nikitenko, A. S. (2019). Modelling of the auroral hiss propagation from the generation region to the ground surface, *Geomagnetism and Aeronomy, 59(5)*, 577-586. https://doi.org/10.1134/S0016793219050074.

Li, H., Wang, C., & Peng, Z. (2013). Solar wind impact on growth phase duration and substorm intensity: A statistical approach. *Journal of Geophysical Research: Space Physics*, *118*, 4270–4278. https://doi.org/10.1002/jgra.50399

Maggs, J. E. (1976). Coherent generation of VLF Hiss. *Journal of Geophysical Research*, *81*, 1707–1724. https://doi.org/10.1029/JA081i010p01707

412 Makita, K. (1979). VLF/LF hiss emissions associated with aurora. *Memories of National Institute of*
413 *Polar Research. Ser. A, 16*, 1–126
414 Manninen, J. (2005). Some aspects of ELF-VLF emissions in geophysical research, *Sodankylä,*
415 *Geophysical Observatory Publication*, *98*, Oulu University Press, Sodankylä, Finland, 177p.
416 [available at http://www.sgo.fi/Publications/SGO/thesis/ManninenJyrki.pdf]
417 Manninen, J., Turunen, T., Kleimenova, N., Rycroft, M., Gromova, L., & Sirviö, I. (2016).
418 Unusually high frequency natural VLF radio emissions observed during daytime in Northern
419 Finland, *Environmental Research Letters, 11*, 124006. https://doi.org/10.1088/1748-
420 9326/11/12/124006
421 **Manninen, J., Kleimenova, N. G., Fedorenko, Yu. V., Gromova, L.I., Nikitenko, A. S., &**
422 **Turunen, T. (2018). Auroral hiss events observed during the declining phase of the 24-th**
423 **solar cycle at two stations separated by 400 km in longitude, *Proc.10th workshop "Solar***
424 ***Influences on Magnetosphere, Ionosphere and Atmosphere",* Primorsko, Bulgaria, June**
425 **4÷8, 2018,67-70 https://doi.org/10.31401/WS.2018.poc**
426 Martin L. H., Helliwell, R. A. & Marks, K. R. (1960). Association between aurora and very low-
427 frequency hiss observed at Byrd Station, Antarctica. *Nature, 187*, 751–753, 1960.
428 https://doi.org/10.1038/187751a0
429 McEwen, D. J., & Barrington, R. E. (1967). Some characteristics of the lower hybrid resonance
430 noise bands observed by Alouette-1 satellite. *Canadian Journal of Physics, 45*(1), 13–19.
431 https://doi.org/10.1139/p67-003
432 McPherron, R. L. (1970). Growth phase of magnetospheric substorms. *Journal of Geophysical*
433 *Research, 75* (28), 5592–5599. https://doi.org/10.1029/JA075i028p05592
434 McPherron, R. L., Russell, C. T., & Aubry, M. P. (1973). Satellite studies of magnetospheric
435 substorms on August 15, 1968: 9. Phenomenological model for substorms. *Journal of*
436 *Geophysical Research, 78*, 3131–3149. https://doi.org/10.1029/JA078i016p03068
437 **Morgan, M. G., (1977). Auroral Hiss on the Ground at L=4, *Journal of Geophysical Research,***
438 ***82 (16)*, 2387-2390. https://doi.org/10.1029/JA082i016p02387.**
439 Morozumi, H. M. (1965). Diurnal variation of auroral zone geophysical disturbances. *Report of*
440 *Ionosphere and Space Research in Japan*, 19, 286–298
441 Nishino, M., Tanaka, Y., Iwai, A., & Kamada, T. (1982). Comparison between the arrival direction
442 of auroral hiss and the location of aurora observed at Syowa station. *Memories of National*
443 *Institute of Polar Research, 22*, 35–45
444 Ozaki, M., Yagitani, S., Nagano, I., Hata, Y., Yamagishi, H., Sato, N., & Kadokura, A. (2008).
445 Localization of VLF ionospheric exit point by comparison of multipoint ground-based
446 observation with full-wave analysis. *Polar Science, 2*(4), 237–249.
447 https://doi:10.1016/j.polar.2008.09.001
448 Pudovkin, M. I., Shumilov, O. I., & Zaytseva, S. A. (1968). Dynamics of the zone of corpuscular
449 precipitation. *Planetary and Space Science, 16*(6), 881–890.
450 https://doi.org/10.1016/0032-0633(68)90112-8
451 Rosenberg, T. J. (1968). Correlated bursts of VLF hiss, auroral light and X-rays. *Planetary and*
452 *Space Science, 16*, 1419–1421. https://doi.org/10.1016/0032-0633(68)90147-5
453 Sato, M., Ayukawa, M., & Fukunisdhi, H. (1980). Conjugacy of ELF-VLF emissions near L = 6.
454 *Journal of Atmospheric and Solar -Terrestrial Physics, 42*(11–12), 911–928.
455 https://doi.org/10.1016/0021-9169(80)90108-7
456 Sazhin, S. S., Bullough, K., & Hayakawa, M., (1993). Auroral hiss: a review. *Planetary and Space*
457 *Science, 41*, 153–166. https://doi.org/10.1016/0032-0633(93)90045-4
458 Sergeev, V., Angelopoulos, V., Kubyshkina M., Donovan, E., Zhou, X.-Z., Runov, A., Singer, H.,
459 McFadden, J., & Nakamura, R. (2011). Substorm growth and expansion onset as observed with
460 ideal ground-spacecraft THEMIS coverage. *Journal of Geophysical Research, 116*, A00I26.
461 https://doi.org/10.1029/2010JA015689

Sonwalkar, V. S., & Harikumar, J. (2000). An explanation of ground observations of auroral hiss: Role of density depletions and meter-scale irregularities. *Journal of Geophysical Research, 105*, 18,867–18,884. https://doi.org/10.1029/ 1999JA000302

Srivastava, R. N. (1976). VLF hiss, visual aurora and the geomagnetic activity. *Planetary and Space Science, 24*, 375–379. https://doi.org/10.1016/0032-0633(76)90050-7

Spasojevic, M. (2016). Statistics of auroral hiss and relationship to auroral boundaries and upward current regions. *Journal of Geophysical Research: Space Physics, 121*, 7547–7560. https://doi.org/10.1002/2016JA022851

Stauning, P. (2013). The Polar Cap index: A critical review of methods and a new approach, *Journal of Geophysical Research: Space Physics, 118*, 5021–5038. https://doi.org/10.1002/jgra.50462

Sulaiman, A. H., Kurth, W. S., Hospodarsky, G. B., Averkamp, T. F., Persoon, A. M., Menietti, J. D., et al. (2018). Auroral hiss emissions during Cassini's Grand Finale: Diverse electrodynamic interactions between Saturn and its rings. *Geophysical Research Letters, 45*, 6782–6789. https://doi.org/10.1029/2018GL077875

Tanaka Y., Haykawa M., & Nishino, M. (1976). Study of VLF auroral hiss observed at Syowa Station, Antarctica. *Memories of National Institute of Polar Research, 13*, 1–58

Tanaka, Y., & Nishino, M. (1988). The propagation of auroral hiss observed on the ground as deduced from direction-finding measurements. *Planetary and Space Science, 36*, 259–269. https://doi.org/10.1016/0032-0633(88)90133-X

Tanskanen, E.I. (2009). A comprehensive high-throughput analysis of substorms observed by IMAGE magnetometer network: Years 1993-2003 examined. *Journal of Geophysical Research, 114*, A05204. https://doi.org/10.1029/2008JA013682.

Troshichev, O. A., Andrezen, V., Vennerstrom, S., & Friis-Christensen E. (1988). Magnetic activity in the polar cap – A new index. *Planetary and Space Science, 36*, 1095–1102. https://doi.org/10.1016/0032-0633(88)90063-3

Troshichev, O. A., Podorozhkina, N. A., Sormakov, D. A., & Janzhura, A. S. (2014). PC index as a proxy of the solar wind energy that entered into the magnetosphere: Development of magnetic substorms. *Journal of Geophysical Research: Space Physics, 119*, 6521–6540. https://doi.org/10.1002/2014JA019940

Ungstrup, E. (1966). Association between VLF emissions & flickering aurora. *Journal of Geophysical Research, 71*, 2395–2396. https://doi.org/10.1029/JZ071i009p02395

Volland, H. (1995). Longwave sferics propagation within the atmospheric waveguide in H. Volland (ed). *Handbook Atmospheric Electrodynamics* (pp. 265–293), Baton Rouge-London-Tokyo: CRC Press Roca

Ye, S.-Y., Fischer, G., Kurth, W. S., Menietti, J.D, & Gurnett, D.A. (2016), Rotational modulation of Saturn's radio emissions after equinox. *Journal of Geophysical Research: Space Physics, 121*, 11,714–11,728. https://doi.org/10.1002/2016JA023281

Figure 1.

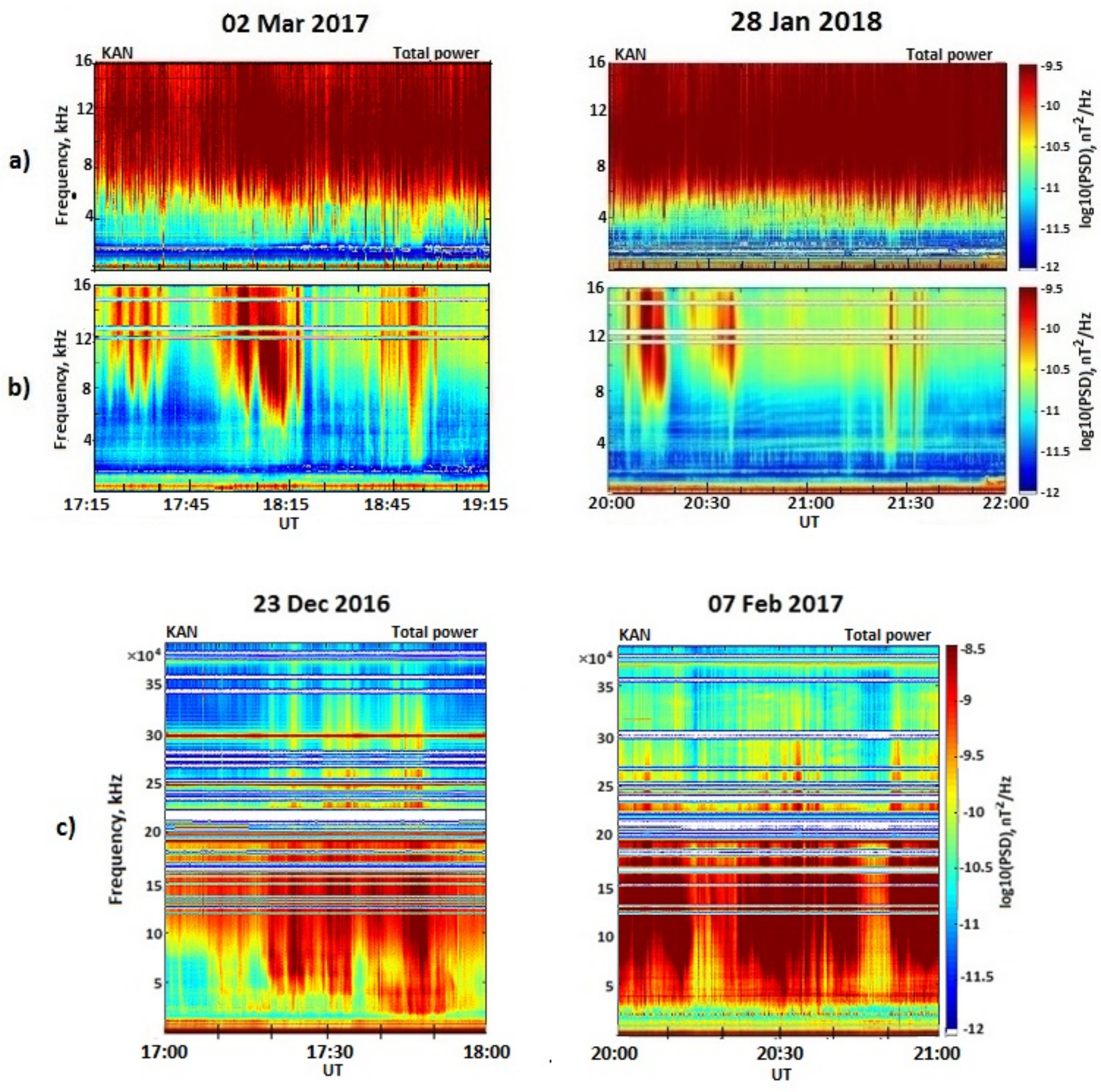
02 Mar 2017
28 Jan 2018
23 Dec 2016
07 Feb 2017
a)
b)
c)
KAN
Total power
Frequency, kHz
log10(PSD), nT²/Hz
UT
17:15
17:45
18:15
18:45
19:15
20:00
20:30
21:00
21:30
22:00
17:00
17:30
18:00

Figure 2.

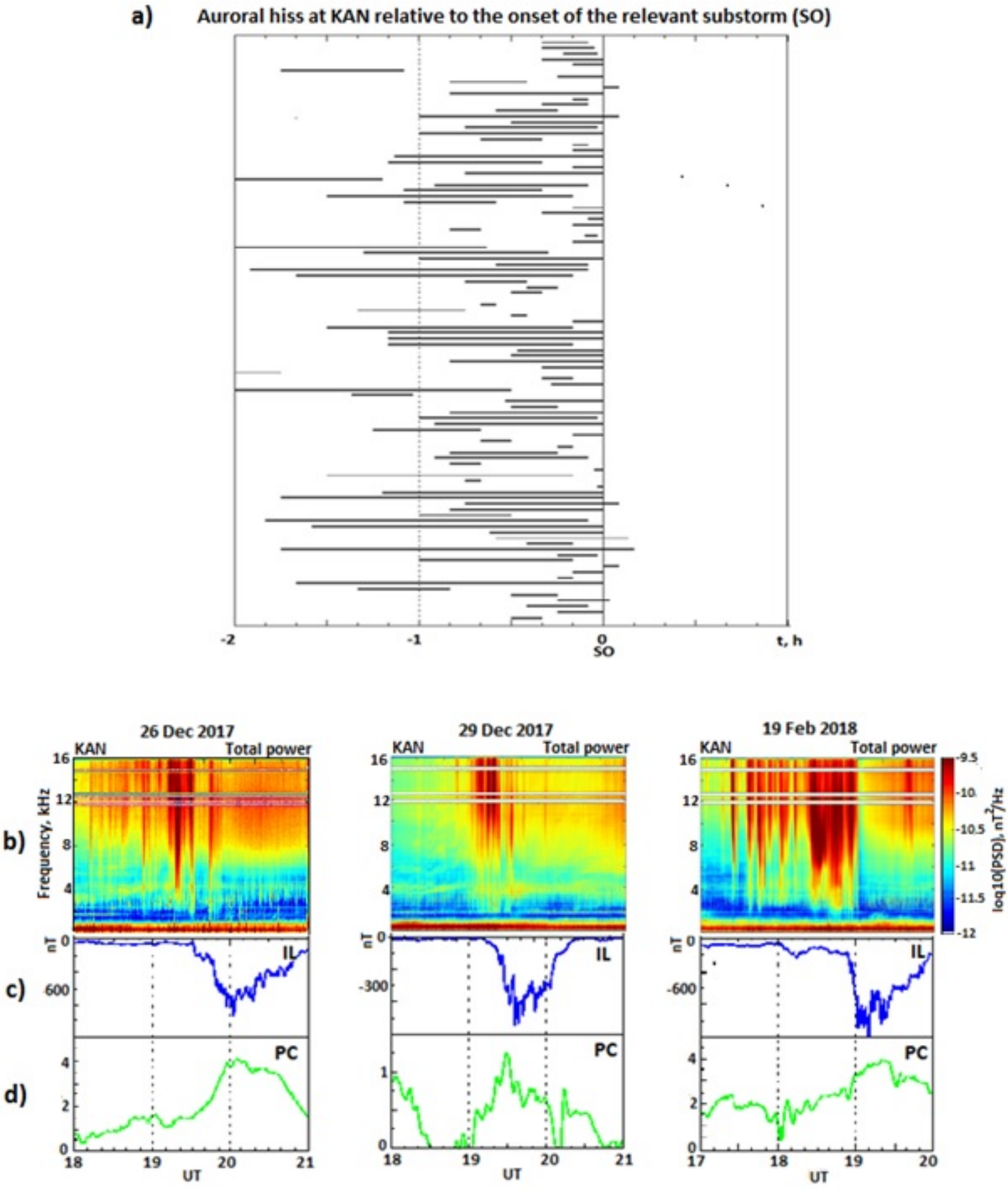
a)
Auroral hiss at KAN relative to the onset of the relevant substorm (SO)
-2
-1
0
SO
t, h
26 Dec 2017
29 Dec 2017
19 Feb 2018
KAN
Total power
b)
Frequency, kHz
16
12
8
4
log10[PSD], nT²/Hz
-9.5
-10
-10.5
-11
-11.5
-12
c)
nT
IL
0
600
-300
-600
d)
PC
2
1
18
19
20
21
17
UT

Figure 3.

23 Dec 2016

a)

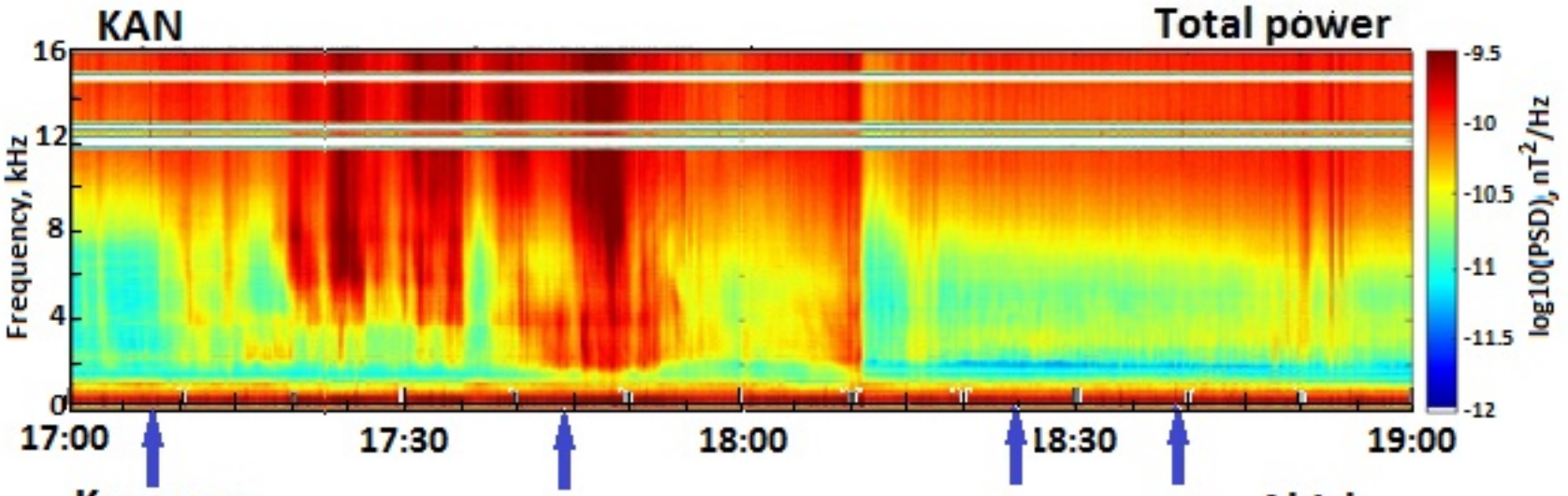

b)

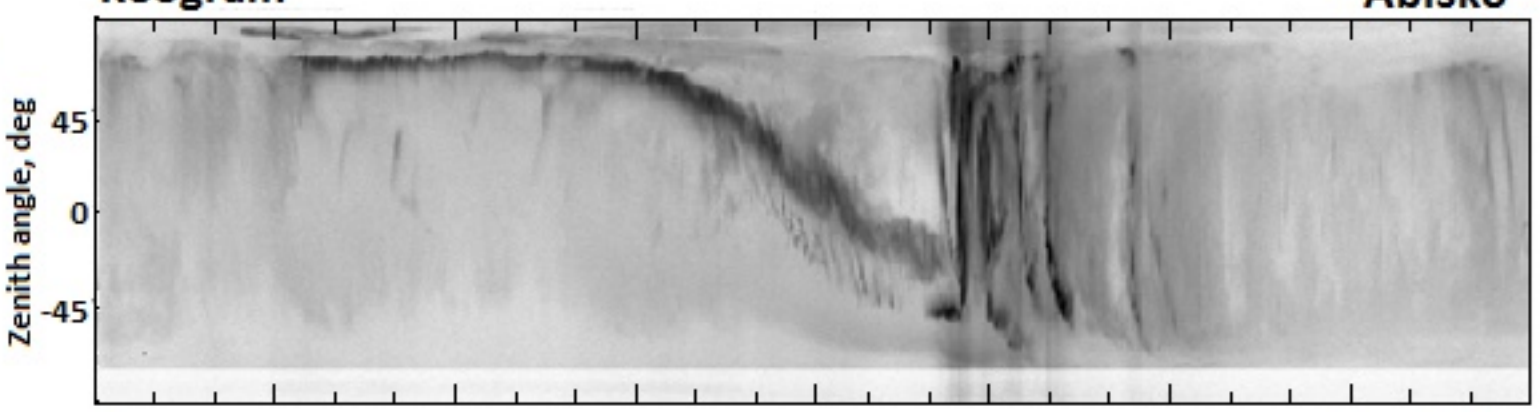

c)

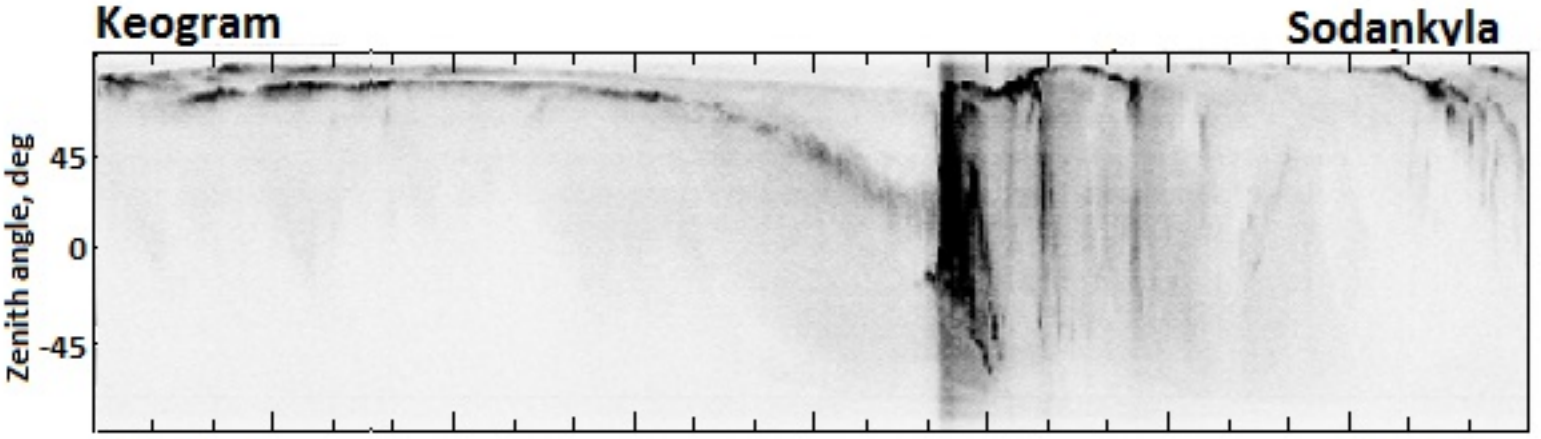

d)

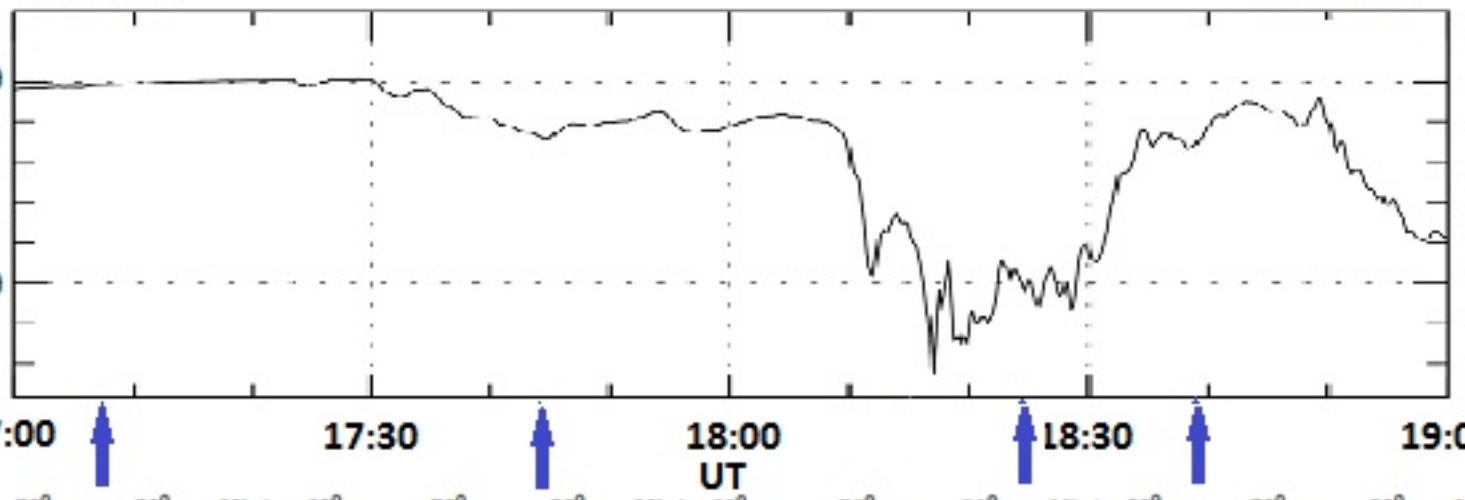

e)